Article:
Wang, J, Han, B, Wang, C orcid.org/0000-0002-4301-3974 et al. (2 more authors) (2022) Study on the effect of graphene/Fe3O4 film on friction and wear performance under water lubrication. Diamond and Related Materials, 130. 109429. ISSN 0925-9635

https://doi.org/10.1016/j.diamond.2022.109429

Study on the Effect of Graphene and Fe_3O_4 Corrosion film on Friction and Wear Performance under Water Lubrication

Jialin Wang[a,b], Bin Han[a]*, Chun Wang[b], Anne Neville[b], Ardian Morina[b]

[a]: School of Materials Science and Engineering,China University of Petroleum (East China), Qingdao, 266555

[b]: Institute of Functional Surface, School of Mechanical Engineering, University of Leeds, LS2 9JT, United Kingdom

*Corresponding author: Bin Han, E-mail: hanbin@upc.edu.cn

Ardian Morina, E-mail: a.morina@leeds.ac.uk

Abastract: In this paper, the corrosion film of Sodium Dodecyl Sulfate (SDS) and graphene aqueous solution was studied. The results showed that the corrosion film is a kind of graphene/Fe_3O_4 film, which has the positive effect of tribological performance under water lubrication. Under the protection of graphene/Fe_3O_4 film, the friction coefficient of steel decreases from 0.41 to 0.17, and the wear scar depth decreases from 2.57 μm to 0.98 μm at load of 2 N. graphene/Fe_3O_4 film exhibits excellent tribological properties under water lubrication due to three reasons. Graphene and Fe_3O_4 are both antifriction materials, which can effectively reduce the friction coefficient and wear rate under water lubrication. The hydrophilicity of graphene/Fe_3O_4 film is significantly improved, which increase the contact area of the water film in the process of water lubrication. The pitting in the corroded surface can continuously collect and release the Fe_3O_4 and graphene, so these antifriction materials can work longer. Under the synergistic effect of the above three aspects, graphene/Fe_3O_4 film had excellent friction reducing and anti-wear effect under water lubrication.

1 Introduction

Industrialization has caused a lot of irreversible pollution to the environment, so many countries are actively looking for environment-friendly technologies. As a new kind of environment-friendly equipment, water-powered rock drill uses distilled water instead of oil as transmission medium, which effectively reduces oil pollution and improves energy utilization[1-3]. However, compared with oil-powered rock drill, the clearance of water-powered rock drill should be kept within 10 μm. Figure 1 shows the core parts of water-powered rock drill. The high-pressure water will leak from the gap between piston and the cylinder. The calculation formula of leakage rate is as follows[4]: $Q=\frac{\pi d h^3 \Delta P}{12 \mu l}$(The flow is assumed to be laminar flow), where ΔP is the pressure difference,

Q is the water leakage rate, d is the piston diameter, h is the clearance between the piston and cylinder, μ is the dynamic viscosity of water, l is the length of the cylinder. From this formula it can be seen that there are two difficulties in the manufacture of water-powered rock drill. Firstly, there is a big difference between the dynamic viscosity coefficient of mineral oil and water, the viscosity coefficient of water is 0.8949×10^{-3} $Pa{\cdot}s$, and the viscosity coefficient of mineral oil is 2.53×10^{-1} $Pa{\cdot}s$. Assuming that other parameters are consistent, the leakage rate of water medium is 280 times that of the oil medium. Secondly, the leakage is proportional to the cubic power of the water-powered rock drill gap. When the water-powered rock drill gap becomes larger due to wear, the leakage will increase rapidly, and the high leakage will lead to the decrease of the service life. Therefore, for the development of water-powered rock drill, the wear between materials under water lubrication should be reduced.

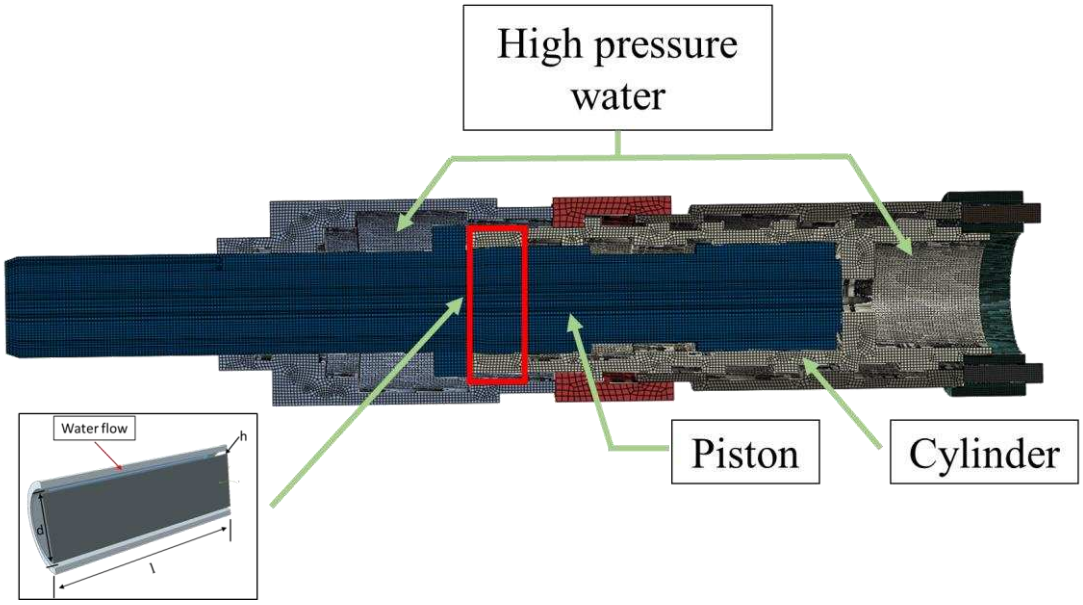

Figure 1 Schematic diagram of core components of water-powered rock drill

The oxide film formed by the tribochemical reaction can effectively reduce the friction coefficient and wear rate[5-7] and Adding anti-friction substances to water can further improve the tribological performance. For example, Sun et al.[8] demonstrated that the addition of MoS_2 in water can form a double-layered tribofilm, which reduces the friction coefficient and wear rate by 37.9%. This double-layered tribofilm consists of oxides produced by tribochemical reaction and deposited MoS_2. Compared with MoS_2,

graphene is considered to be a more advanced water-based additive[9-11] . Kim et al.[12] measured the friction force of fluorinated, hydrogenated, oxidized graphene and pure graphene by friction force microscopy measurements. The results showed the friction force of pure graphene was one seventh of the former. According to Kim et al.[4] experimental results, the friction and wear resistance of graphene should be better than that of graphene oxide. However, the tribological properties of graphene as a water-based additive were lower than that of graphene oxide[13-16]. This is due to the fact that graphene is a hydrophobic material, which will agglomerate in water, and it is difficult for graphene to enter the gap between two friction surfaces. So surfactant is added to graphene solution to improve its dispersion in water[17, 18]. Liang[19] added the Triton X-100 to graphene aqueous solution and found that the friction coefficient and wear rate are lower than those of graphene oxide solution. Therefore, for graphene, the most important thing is to make it into the gap of the friction pair.

Fe_3O_4 mixed with MoS_2 or rGO is used as an additive for water or mineral oil in the field of antifriction and wear resistance[20-25]. According to the relevant research of Zheng et al.[24], the friction coefficient and wear rate of MoS_2&Fe_3O_4 mixed solution are lower than that of single Fe_3O_4 solution. By analyzing the magnetism of Fe_3O_4, Xu et al.[22] believe that the magnetic Fe_3O_4 can adsorb the surrounding friction reducing substances such as MoS_2 and rGO during the friction process.

In this paper, the double-layered tribofilm was prepared by using the characteristics of Fe_3O_4 adsorbbing anti-friction materials. Graphene/Fe_3O_4 film were prepared on the steel surface after the corrosion of SDS and graphene aqueous solution. In this way, a large amount of graphene can enter the gap during sliding test. The friction and wear properties of graphene/Fe_3O_4 film were investigated under water lubrication. Through observing the wear scar, the anti-friction and wear resistance mechanism of graphene/Fe_3O_4 film was explored.

2 Experimental process

2.1 Graphene/Fe_3O_4 film preparation

Both SDS and graphene used in this experiment were provided by Sigma Aldrich. 1*g* graphene and 1*g* SDS were added into 100 *g* distilled water, and then the graphene aqueous solution containing SDS was stirred for 1 hour with a magnetic stirrer. The aqueous solution was treated with ultrasonic wave for 30 minutes to make graphene fully dispersed in the aqueous solution. Before the corrosion, the samples were ultrasonic cleaned with acetone for 30 minutes and then placed into the prepared aqueous solution for 4 hours, 12 hours, 24 hours and 48 hours respectively. All the samples were AISI 52100. During the corrosion process, the solution temperature was kept at 25 ℃. After the corrosion process, the samples were dried in an oven and rinsed with distilled water.

2.2 Friction and wear test

All tribological tests were carried out on the Mini Traction Machine (MTM) tribometer produced by PCS Instruments, where a 19.05 *mm* diameter ball was loaded rubbing with a 46 *mm* diameter disc (as shown in Figure 2). At the beginning of the test, distilled water was added to the MTM. The ball and disc were completely immersed in distilled water during the experiment. The load was 2-8 *N* and the relative sliding speed was 2 m/s for 3 hours, slide to roll ratio was 200 %. To ensure the reliability and accuracy of the test, the results were the average of three times of the test.

White light interferometer (NP-Flex, Bruker, USA) was used to measure the depth and width of the wear scar. The software Vision 64 generated the 3D profile of the wear scar, where the magnification lens used was 10×. The roughness of the corroded surface was also measured by Vision 64. The surface morphology and chemical elements of wear marks were observed by Scanning Electron Microscopy (SEM, Fei quanta, FEG 250) equipped with EDS. The composition of the corrosion film and the wear scar was carried out by Raman spectroscopy. The samples were exposed for 10 *s* at 488 *nm* wavelength with 100 % laser power. A small spot size of 10×10 μm was chosen to detect the pitting. The wettability of samples was evaluated by a contact angle meter (Dataphysics OCA 15EC, Germany). Contact angles were tested by fitting water drops (1 μL) with the Laplace-Young equation.

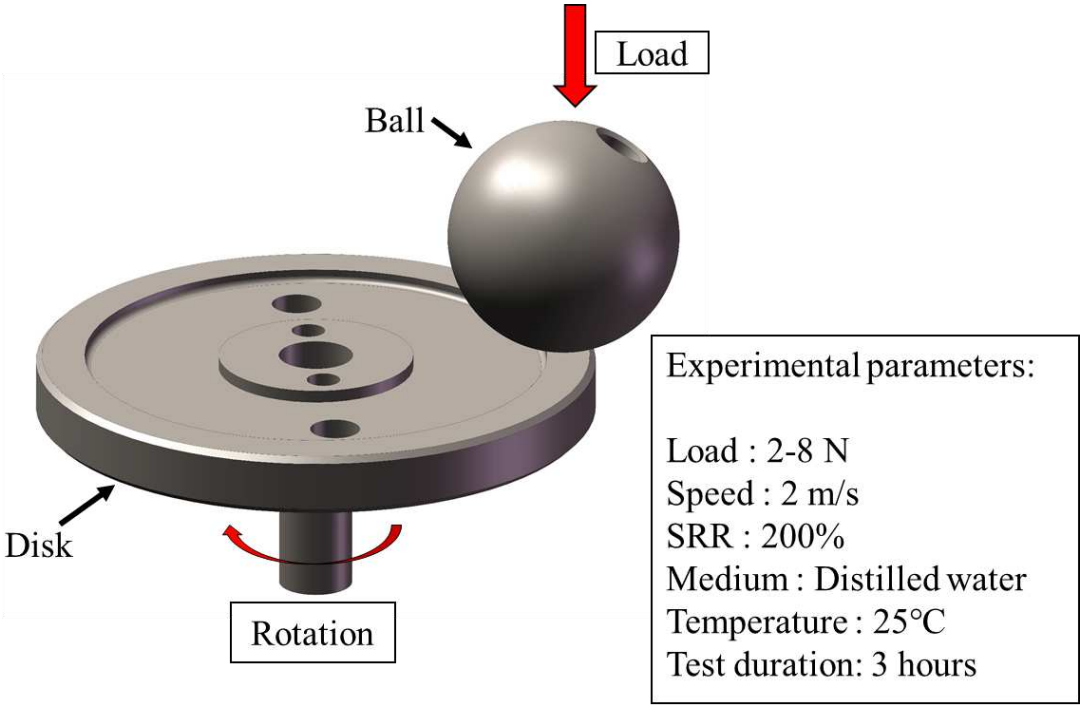

Figure 2 Configuration of MTM ball-on-disk tribometer and the corresponding experimental parameters.

3 Results and discussion

3.1 Surface morphology and composition of graphene/Fe_3O_4 film

The surface morphology and Carbon and Oxygen elements distribution of the corrosion film are shown in Figure 3. Carbon mainly comes from graphene and the oxygen comes from iron oxidation. At the beginning of corrosion, pitting was observed on the surface of the sample (as shown in Figure 3 (a)). The size of the pits is between 10-30 μm. From the EDS shown in Figure 3 (a), carbon is mainly distributed inside the pits. With the increase of immersion time, the sample surface continued to oxidize (as shown in Figure 3 (b)). These oxides were seen to be evenly distributed on the surface. When the immersion time was 24 hours, the surface oxidation was enhanced and the graphene was evenly distributed on the surface, (as shown in Figure 3 (c)). The surface of the sample immersed for 48 hours was completely oxidized. In general, The EDS results indicate that the oxides formed on the surface were mixed with graphene. Moreover, with the increase of immersion time, the distribution of graphene in the oxide film tended to be uniform.

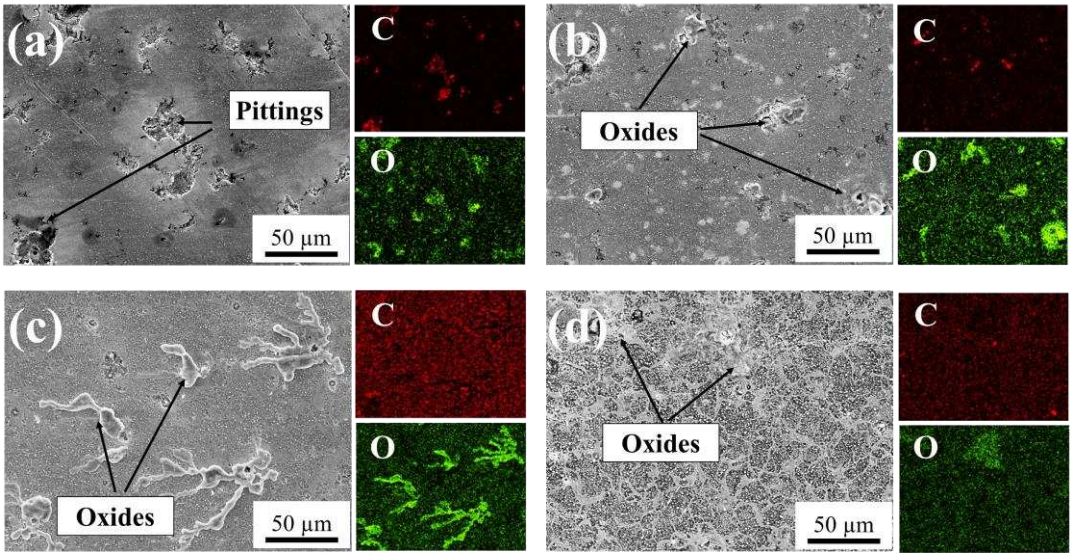

Figure 3 SEM images of different immersion time (500 ×) and the corresponding distribution of C and O elements, a) 4 hours, b) 12 hours, c) 24 hours, d) 48 hours

Figure 4 shows high-magnification SEM images of sample surfaces following different immersion times. From Figure 4, it can be clearly seen that the flat area of the sample surface gradually changes into a network structure. In fact, these network structures are the grain boundaries of the samples, and their sizes are 3-10 μm. As the network structure composed of grain boundaries is higher than other regions, it can be hypothesized that the anti-friciton materials, like graphene and oxides, will be easily stored in this network structure..

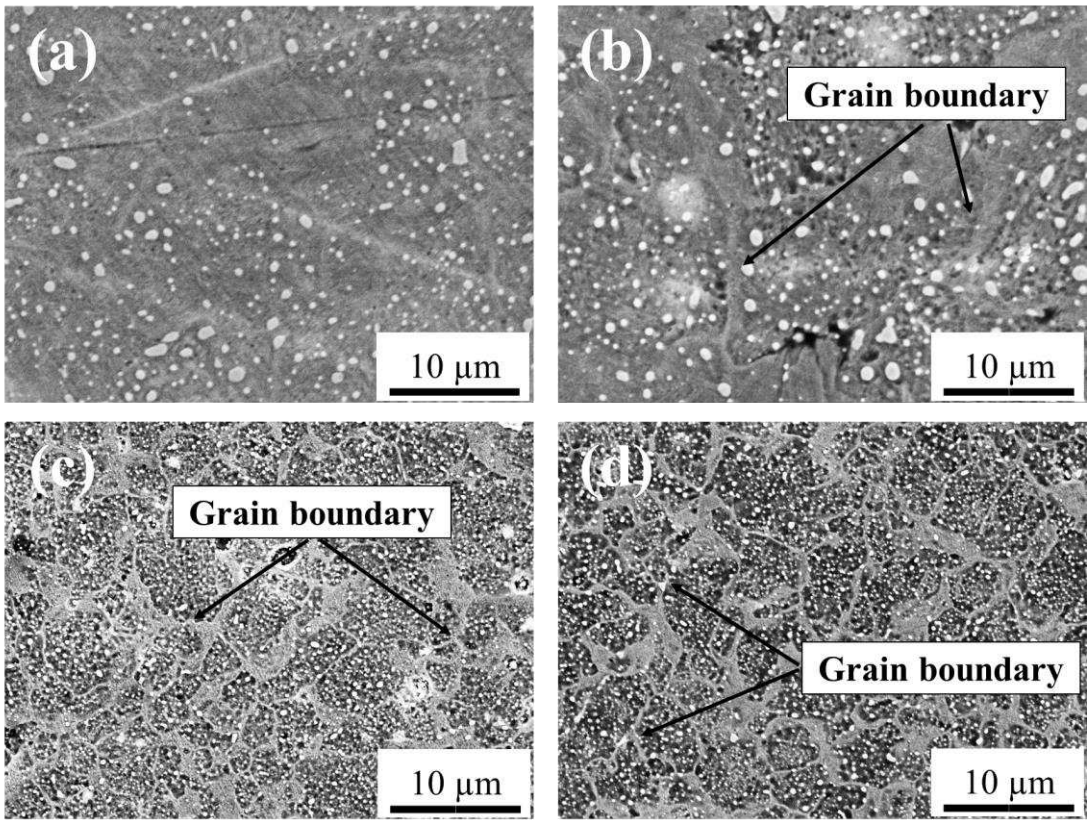

Figure 4 SEM image of flat area of sample with different immersion time (1000 ×), a) 4 h, b) 12 h, c) 24 h, d) 48 h

From the above analysis, it can be seen that the steel surface has been oxidized and graphene deposited on the oxidized surface. To explore the thickness of oxides/graphene film, Figure 5 shows sample cross-sections and their corresponding EDS maps. When the immersion time is 4 hours, graphene has begun to deposit on the surface, but there is no oxygen element on the sample surface. When the immersion time increase to 12 hours, the sample surface is obviously oxidized, and the graphene film increases from 0.35 *μm* to 0.9 *μm* (as shown in Figure 5 (b)). According to Figure 5 (c) and Figure 5 (d), with the continuous increase of immersion time, the thickness of deposited graphene film and oxide film gradually increases. When the immersion time is 48 hours, the distribution of oxide film and graphene film on the sample surface is uniform. This shows that graphene and oxide are mixed together. Previous reports have shown that graphene is difficult to adsorb on steel surfaces [19], but Fe_3O_4 film changes the surface morphology and properties of steel, making graphene more easily deposited

on its surface[22]. The more intense the surface oxidation is, the more graphene deposition is achieved. As a result, the thickness of graphene and oxide film increased with immersion time.

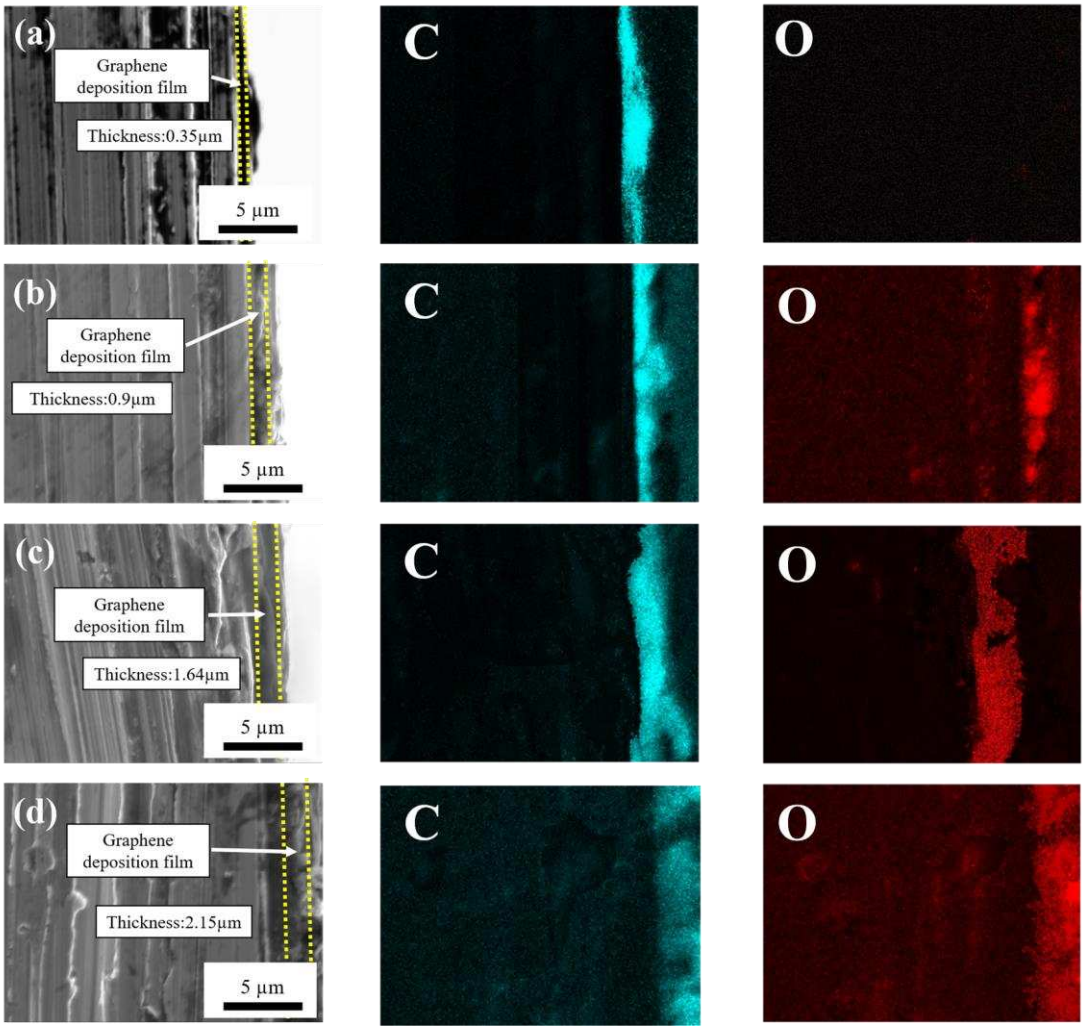

Figure 5 SEM images of cross-sections with different immersion time and corresponding distribution diagrams of C and O elements. a) 4 hours, b) 12 hours, c) 24 hours, d) 48 hours

In order to identify the type of oxides and confirm the deposition of graphene, Figure 6 exhibits the Raman spectra obtained from the original graphene powder, the AISI-52100 steel substrate and the corrosion film. The G and D peaks are characteristic peaks of graphene[26]. The D peak, located at 1350 cm^{-1}, relates to the defect of graphene[27]. The G peak, located at 1580 cm^{-1}, is caused by the in-plane vibration of sp^2 carbon atom. In the Raman spectra of graphene, the I_D/I_G can be used to characterize the sp^3/sp^2

bonding ratio[28, 29]. Compared with the initial graphene (shown in Figure 6 (a)) and AISI-52100 substrate (shown in Figure 6 (b)), the Raman spectrum of corroded surface confirms the formation of Fe_3O_4 and graphene deposition . The Raman peak at 655 cm^{-1} corresponds to Fe_3O_4[30-32], which demonstrates the graphene/Fe_3O_4 film was prepared on the AISI-52100 surface sucessfully.

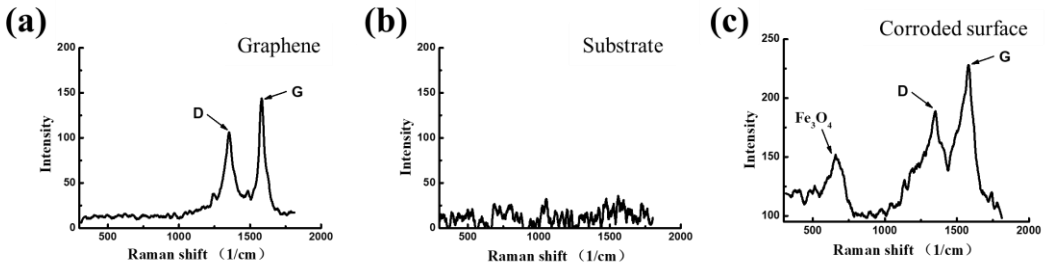

Fig. 6 Raman spectra of , a) the original graphene, b) the steel substrate, c) the corroded surface after 24 hours immersion

3.2 Friction and wear of the graphene/Fe_3O_4 film under water lubrication

The friction coefficient under water lubrication is shown in Figure 7. The friction coefficient decreases significantly as the graphene/Fe_3O_4 film covers on the steel surface. According to the results of Figure 7 (a), after immersion for more than 12 hours, the friction coefficient of the corroded surface is stable at around 0.2. Compared with the sample without immersion, the friction coefficient decreased by 60% when the sample immersed for 24 hours. This significant reduction in friction coefficient can be attributed to the graphene/Fe_3O_4 film[33-35]. For the samples immersed more than 12 hours, enough graphene/Fe_3O_4 film was covered on the surface, reducing the friction coefficient.

According to the lubrication theory, the lubrication regimes can be divided into three main types: boundary lubrication, mixed lubrication and hydrodynamic lubrication. The value of λ is used to assessthe lubrication regime under different tribological parameters: when $\lambda < 1$, it is boundary lubrication; when $1 < \lambda < 3$, it is mixed lubrication; when $\lambda > 3$, it is fluid lubrication. The value of λ is calculated as follows:

$$\lambda = \frac{h_0}{\sqrt{R_{q1}^2 + R_{q2}^2}} \tag{3.1}$$

Where the h_0 is the water film thickness, Rq_1 and Rq_2 are the roughness of the two surfaces, λ is the ratio of the water film thickness to the roughness of the two contact surfaces. The h_0 can be calculated using the Hamrock-Dowson equation[36, 37]:

$$h_0 = 3.63\left(\frac{U_e\eta_0}{E_rR'}\right)^{0.68}(\alpha E')^{0.49}\left(\frac{W}{E_rR'^2}\right)^{-0.073}\left(1 - e^{-0.68k}\right)R' \tag{3.2}$$

Where U_e is the relative sliding velocity, η_0 is the viscosity coefficient of water, R' is the equivalent radius of curvature, E_r is the equivalent elastic modulus, and α is pressure-viscosity coefficient. According to Jon's researche[38], the pressure-viscosity coefficient of water changed little at room temperature, so the α=1. Considering the tribological conditions in this study (load 2 *N* and speed 2 *m/s*), the thickness of the water film is 15 nm and the λ ratio is 0.035, showing that the tests are run in boundary lubrication regime. Boundary lubrication means that the water film does not separate the contact points of the friction pair, and only a small part of the water film is involved in friction reduction and wear resistance. Hence, the friction performance is mainly provided by thecorrosion graphene/Fe_3O_4 film.

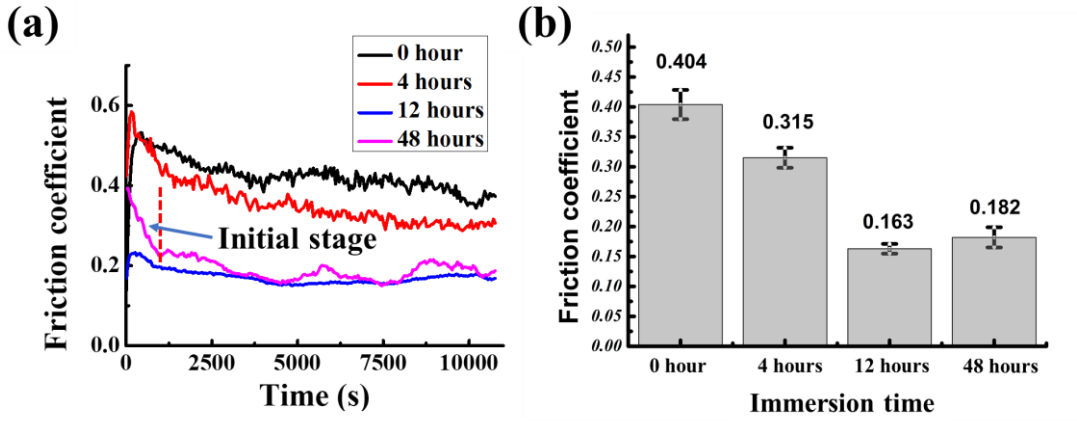

Figure 7 Friction coefficient of samples immersed for 4 hours, 12 hours and 48 hours under water lubrication, load 2 *N*, speed 2 *m/s*, a) friction coefficient-time curve, b) average value of friction coefficient

Figure 8 shows the wear scar profiles of different graphene/Fe_3O_4 film. The widths of wear scar changed little, but the depth of wear mark is significantly higher with the increase of immersion time. Based on Hertzian contact theory, under 2 *N* the maximum contact pressure is about 393 *MPa* and Hertzian contact zone is 98 μm (diameter), so the initial width of wear scar should be 98 μm. With the aggravation of wear, the width of wear scar increases to 780-970 μm (as shown in Figure 8 (a)-(d)). Due to a lack of graphene/Fe_3O_4 film the depth of the wear scar reaches 2.57 μm when the immersion time is 0 hour. With immersion time increasing to 4 hours, the depth of the wear scar reduced to 1.90 μm because graphene/Fe_3O_4 film works. As the content of Fe_3O_4 and graphene are low graphene/Fe_3O_4 film are worn off during sliding test. But when the immersion time increases 12 hours enough graphene/Fe_3O_4 film forms on the surface of the sample and the depth of wear scar is minimum (0.98 μm). For the sample immersed for 48 hours the depth of wear scar increases to 1.2 μm as the center of graphene/Fe_3O_4 film is worn through.The width of worn through areas is 0.148 *mm*. As shown in Figure 7 (a), this failure area also reduces the friction coefficient slightly. Generally speaking, graphene/Fe_3O_4 film can effectively protect the steel surface from severe wear.

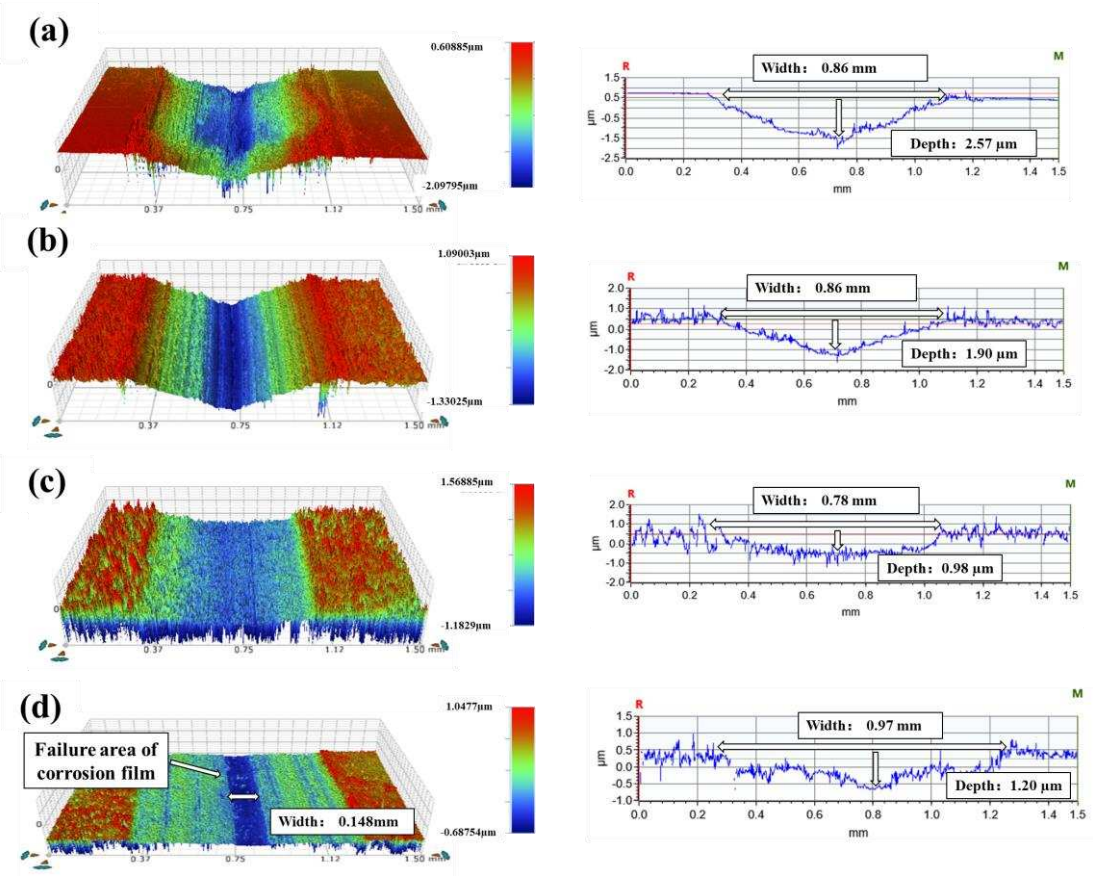

Figure 8 Wear scar 3-D profiles of samples with different immersion time, 2 *N*, 2 *m/s*, a) 0 *h*, b) 4 *h*, c) 12 *h*, d) 48 *h*.

Figure 9 shows the friction coefficient of graphene/Fe_3O_4 film at the load of 4-8 *N*. The graphene/Fe_3O_4 film exhibits low friction coefficient at load of 4 *N*. But when the load increase to 6 *N*, the friction coefficient be divided into two stages. The initial stage is similar to that of 4 *N*. The graphene/Fe_3O_4 film protects the substrate and its friction coefficient exhibites low value accordingly. Meanwhile, at this stage, the graphene/Fe_3O_4 film is gradually worn and eventually fails. After 4800 *s*, the corrosion graphene/Fe_3O_4 film is failed completely due to severe wear, which also led to its friction coefficient rising to 0.5. The corrosion film has no effect on friction and wear resistance at load of 8 *N*. Therefore, the friction coefficient is always at a high level. Figure 9 (b) shows the average friction coefficient at different loads. The friction coefficient increases from 0.25 to 0.5 when the load changes from 4N to 8N. Generally speaking, the graphene/Fe_3O_4 film can reduce the friction under low load. With the

increase of the load, the graphene/Fe_3O_4 film will be worn off, resulting in a high friction coefficient.

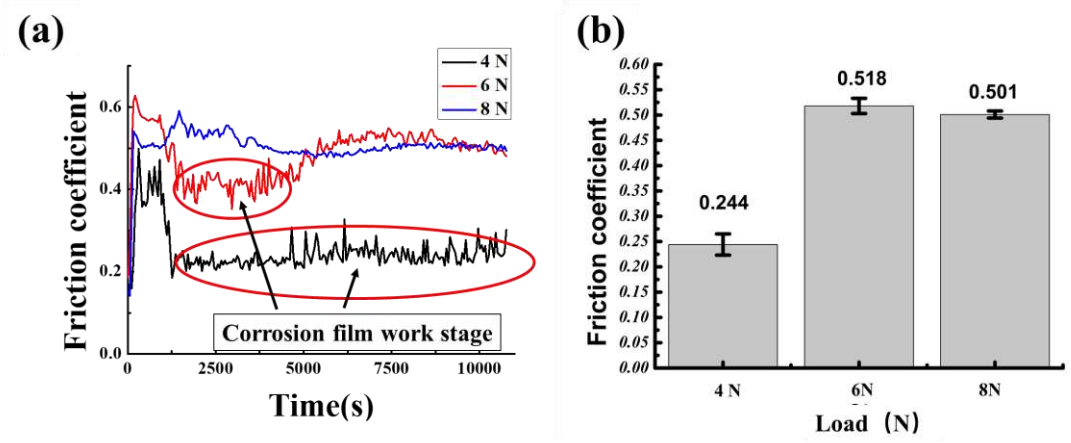

Figure 9 Friction coefficient of the sample immersed for 12 hours at load of 4 *N*, 6 *N* and 8 *N*; a) Variation of friction coefficient with time; b) Average friction coefficient.

The 3-D morphology of the surface with the load of 4 *N*, 6 *N* and 8 *N* is shown in Figure 10. Compared with 6 *N* load and 8 *N* load, the wear mark under 4 *N* is flat. Similar with load of 2 *N* the wear scar depth of 4 *N* is only 1.12 μm. So the graphene/Fe_3O_4 film can effectively protect the steel surface at load of 4 *N*. But when the load increases to 6-8 *N*, the depth of wear scar increases sharply. Figure 10 (b) and Figure 10 (c) show that the depth of wear scar is 4.1 μm for 6 *N* and 4.4 μm for 8 *N*, and the width is 1.07 *mm* and 1.26 *mm*, respectively. Although the graphene/Fe_3O_4 film of 6 *N* load sample can reduce friction and wear resistance during 1800-4800 *s*, the final wear scar depth of 6 *N* is not significantly reduced compared with that of 8 *N*. So once the protection of graphene/Fe_3O_4 film failed, the wear depth increases rapidly. Overall, the variation of wear rate is consistent with the variation of friction coefficient under load of 4-8 *N*. In the case of low load, graphene/Fe_3O_4 film is shown to reduce friction coefficient and the wear. When graphene/Fe_3O_4 film wear off, the friction coefficient and the wear increased significantly.

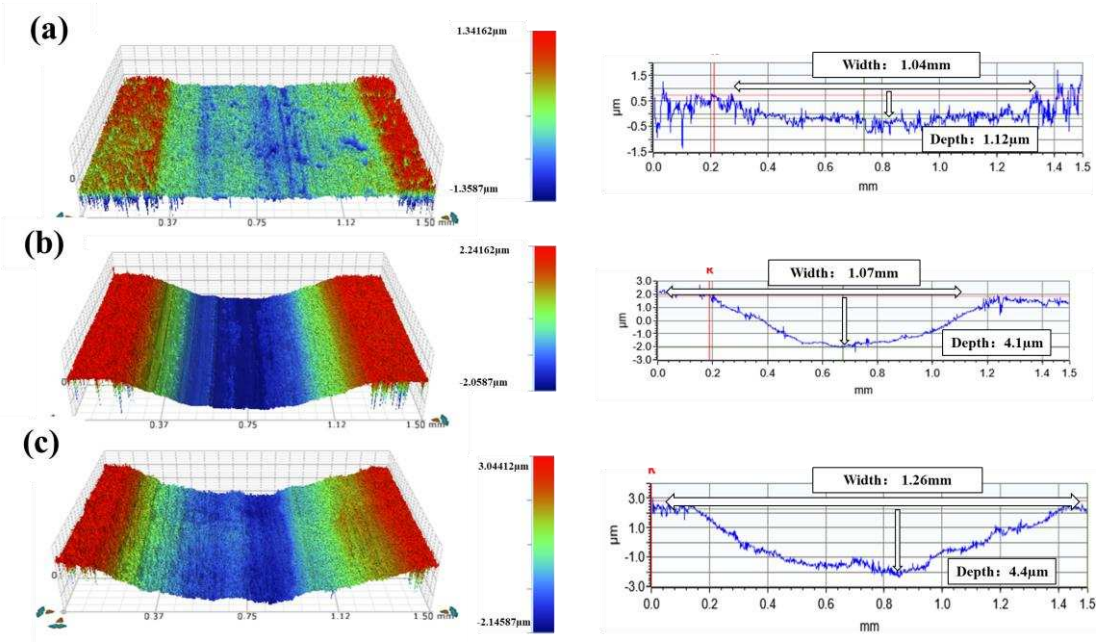

Figure 10 Wear scar surface profile of the sample after soaking for 12 hours under different loads, a) 4N, b) 6N, c) 8N

Figure 11 shows the SEM images of wear scar corresponding to Figure 8. The wear scar morphology of the sample immersed for 4 hours is similar to that of the sample without immersion. Due to the same material used for the ball and disc the adhesive wear occurs during the sliding test. Figure 11 (a) shows the furrows, the adhesive wear area. The oxide (the dark area) formed during sliding test. Similar to the sample without immersion, the surface of the sample immersed for 4 hours is mainly abrasive wear and adhesive wear. The formation of oxide indicates that the oxidation reaction takes place in the state of water lubrication. The oxide film can reduce the friction coefficient, so the friction coefficient of the samples gradually decreases (shown in Figure 7 (a)). Due to the protection of graphene/Fe_3O_4 film, less furrows are exhibited on worn surface. The pittings shown in Figure 11 (c) can collect and store graphene and Fe_3O_4 debris, which can reduce the friction coefficient and wear. After immersed for 48 hours, the worn surface of the sample can be divided into two regions. The central region corresponds to graphene/Fe_3O_4 film failure area in Figure 8 (d). The formation of this region is related to the serious wear of graphene/Fe_3O_4 film, which also leads to higher friction coefficient compared with the sample covered with intact graphene/Fe_3O_4 film

(As shown in Figure 7 (a) bule and purple curve). Due to graphene/Fe_3O_4 film, the friction coefficient decreased to about 0.2. The results show that graphene/Fe_3O_4 film can effectively avoid adhesive wear and reduce abrasive wear, which can protect the surface of the sample.

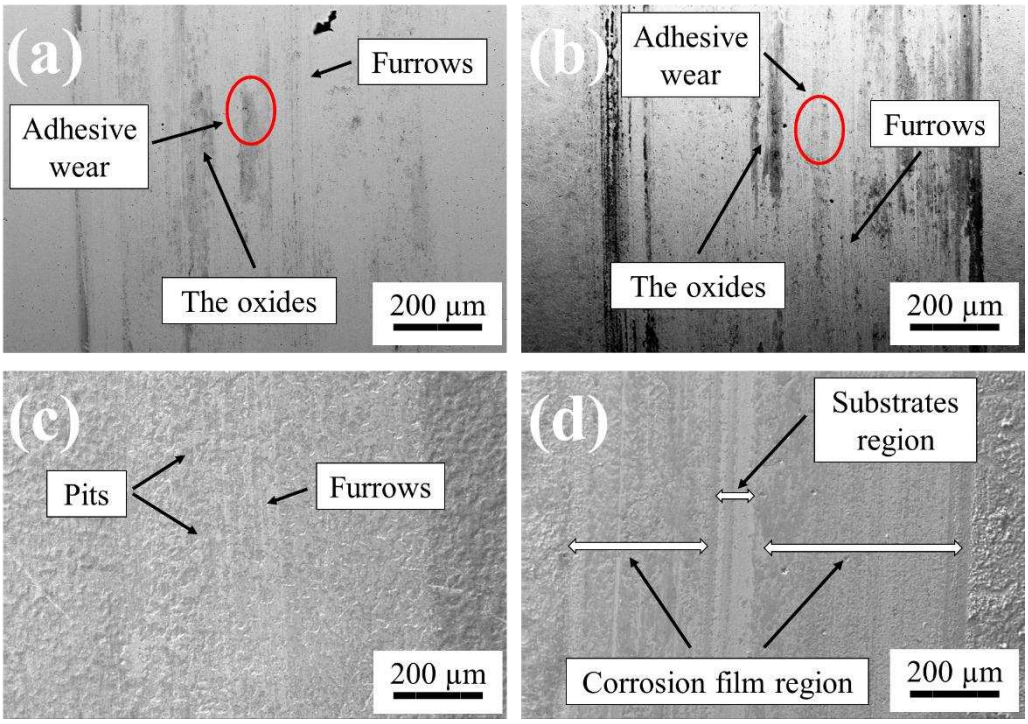

Fig. 11 SEM images of friction surfaces with different immersion time(250×), a) 0 h, b) 4 h, c) 12 h, d) 48 h.

3.3 Anti-friction and wear mechanism of graphene/Fe_3O_4 film

Figure 12 shows the contact angle between distilled water and graphene/Fe_3O_4 film. Wettability has a significant effect on the tribological properties due to the competition between attractive van der Waals interactions and wettability dependent repulsive hydration interactions[39, 40]. With the increase of immersion time, the contact angle between steel surface and water gradually decreases. When the immersion time is more than 12 hours, the contact angle is stable at about 54 degrees. Compared with the original sample surface, the corrosion film is easier to be wetted. For the use of graphene in antifriction and wear resistance, wettability is very important[17, 18]. Low wettability can make graphene enter the gap between friction pairs, so that graphene

could play the role of friction reduction and wear resistance.

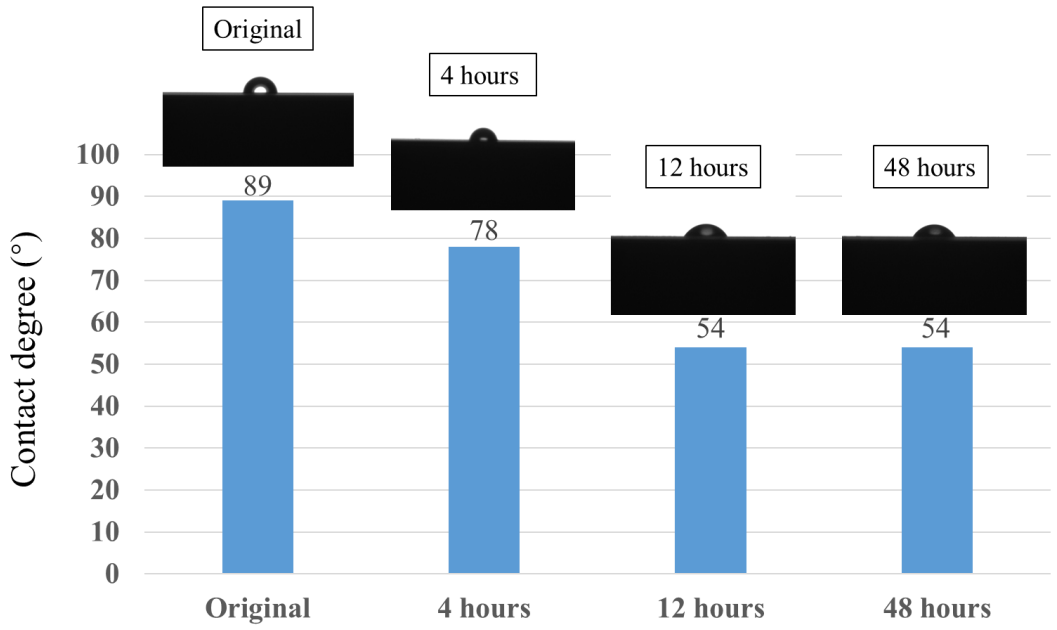

Figure 12 The change of contact angle with immersion time in aqueous solution of graphene containing SDS

Figure 13 shows the C and O distribution on the worn surface when the immersion time is 4 hours and 12 hours. The results show that the wear scars soaked for 4 hours mainly contain oxides. These oxides are the products of tribochemical reactions. However, according to the distribution of C, there is no graphene deposited on the wear scar, which means the original graphene deposited on the surface has been washed off during sliding test. Figure 13 (b) shows (12 hours) that C and O in the worn surface are distributed along the friction direction and they are mainly distributed in the pittings. During the sliding test, graphene/Fe_3O_4 film falled off. These exfoliated graphene and Fe_3O_4 were recollected by pitting[41]. Graphene and Fe_3O_4 in the pitting will be continuously released to the surrounding area, which makes the contact area continuously protected by these antifriction materials. Compared with smooth surface, the collection and release mechanism of graphene and Fe_3O_4 improves the utilization rate of antifriction materials.

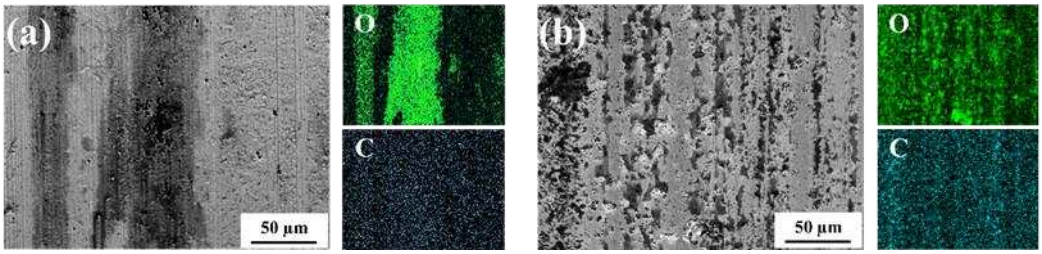

Figure 13 Surface morphology and distribution of C and O elements at the wear marks of samples with different immersion time, a) 4h, b) 24h

Figure 14 shows the Raman spectrum of the pittings within the wear scar. The Raman spectra proves that the pittings contain graphene and Fe_3O_4. These graphene and Fe_3O_4 come from the exfoliated graphene/Fe_3O_4 film. Compared with the original graphene, the D peak of graphene in the wear scar is enhanced. The I_D/I_G in wear mark is higher than that of original deposited graphene, which means an increase in the defect and disordering of graphene[42]. Raman spectra confirmed that graphene and Fe_3O_4 are stored in the pitting during the sliding test.

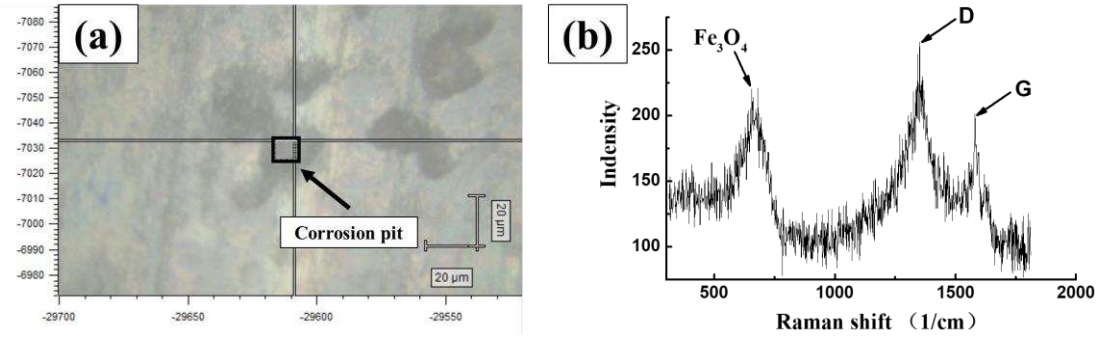

Figure 14 Raman spectra of pittings in wear marks, a) Testing position of Raman spectrum, b) Corresponding Raman spectrum

4 Conclusion

The Fe_3O_4 can absorb the graphene to from graphene/Fe_3O_4 film. Through the corrosion of graphene/SDS aqueous solution, graphene/Fe_3O_4 film could be formed on the steel surface. The tribological test showed that graphene/Fe_3O_4 film can reduce the friction

coefficient and wear under water lubrication. If the graphene/Fe_3O_4 film is not damaged, the friction coefficient is about 0.2. If the corrosion film is worn off, the friction coefficient will increase to about 0.5, and the wear rate will also be greatly increased. Further research shows that the graphene/Fe_3O_4 film can play a role in reducing friction and wear mainly due to the following three points: Firstly, both graphene and Fe_3O_4 are antifriction material. During the sliding test, graphene and Fe_3O_4 can enter the gap between the friction pairs to reduce the friction coefficient and wear. Secondly, the increase of wettability of the corroded surface makes more water effect on the contact surface. In the process of water lubrication, the increase of water film area will reduce friction and wear. Thirdly, the rough surface after corrosion can collect the Fe_3O_4 and graphene which fall off from the graphene/Fe_3O_4 film. The Fe_3O_4 and graphene collected in the pitting can be continuously released to the surrounding area. This collection-release mechanism improves the utilization of antifriction materials (graphene and Fe_3O_4). Under the synergistic effect of the above three aspects, t graphene/Fe_3O_4 film exhibits excellent tribological properties under water lubrication.

Reference

[1] Q. Wang, F. Zhou, Z. Zhou, Y. Yang, C. Yan, C. Wang, W. Zhang, L.K.-Y. Li, I. Bello, S.-T. Lee, Influence of Ti content on the structure and tribological properties of Ti-DLC coatings in water lubrication, Diamond and Related Materials 25 (2012) 163-175.

[2] M. Kalin, S. Novak, J. Vižintin, Surface charge as a new concept for boundary lubrication of ceramics with water, Journal of Physics D: Applied Physics 39(15) (2006) 3138-3149.

[3] A. Tomala, A. Karpinska, W. Werner, A. Olver, H. Störi, Tribological properties of additives for water-based lubricants, Wear 269 (2010) 804-810.

[4] H. Müller, B. Nau, Fluid Sealing Technology: Principles and Applications, 1998.

[5] B. Kohlhauser, M.R. Ripoll, H. Riedl, C.M. Koller, N. Koutna, A. Amsüss, H. Hutter, G. Ramirez, C. Gachot, A. Erdemir, P.H. Mayrhofer, How to get noWear? – A new take on the design of in-situ formed high performing low-friction tribofilms, Materials & Design 190 (2020) 108519.

[6] Y. Xu, E. Hu, K. Hu, Y. Xu, X. Hu, Formation of an adsorption film of MoS2 nanoparticles and dioctyl sebacate on a steel surface for alleviating friction and wear, Tribology International 92 (2015) 172-183.

[7] A. Khan, S.R. Yasa, R. Gusain, O.P. Khatri, Oil-miscible, halogen-free, and surface-active lauryl sulphate-derived ionic liquids for enhancement of tribological properties, Journal of Molecular Liquids 318 (2020) 114005.

[8] J. He, J. Sun, Y. Meng, H. Tang, P. Wu, Improved lubrication performance of MoS2-Al2O3 nanofluid through interfacial tribochemistry, Colloids and Surfaces A: Physicochemical and

Engineering Aspects 618 (2021) 126428.
[9] Y. Liu, X. Ge, J. Li, Graphene Lubrication, Applied Materials Today 20 (2020).
[10] H.-J. Kim, D.-E. Kim, Water Lubrication of Stainless Steel using Reduced Graphene Oxide Coating, Scientific Reports 5 (2015) 17034.
[11] D. Shin, D.-E. Kim, Frictional behavior between silicon and steel coated with graphene oxide in dry sliding and water lubrication conditions, International Journal of Precision Engineering and Manufacturing-Green Technology 3 (2016) 91-97.
[12] K. Jae Hyeon, S. Kwon, I.-S. Byun, J. Choi, B. Park, Y.-H. Kim, J. Park, Nanotribological Properties of Fluorinated, Hydrogenated, and Oxidized Graphenes, Tribology Letters 50 (2013).
[13] X. Hongmei, B. Jiang, J. Dai, C. Peng, C. Li, Q. Li, F.-S. Pan, Tribological Behaviors of Graphene and Graphene Oxide as Water-Based Lubricant Additives for Magnesium Alloy/Steel Contacts, Materials 11 (2018) 206.
[14] J. Zhao, Y. He, Y. Wang, W. Wang, L. Yan, J. Luo, An investigation on the tribological properties of multilayer graphene and MoS2 nanosheets as additives used in hydraulic applications, Tribology International 97 (2016) 14-20.
[15] Y. Wu, L. Zeng, T. Ren, E.G. De Vries, E. Van Der Heide, The emulsifying and tribological properties of modified graphene oxide in oil-in-water emulsion, Tribology International 105 (2016).
[16] H. Mungse, O. Khatri, Chemically Functionalized Reduced Graphene Oxide as a Novel Material for Reduction of Friction and Wear, The Journal of Physical Chemistry C 118 (2014) 14394–14402.
[17] T. Drobek, N. Spencer, Nanotribology of Surface-Grafted PEG Layers in an Aqueous Environment †, Langmuir : the ACS journal of surfaces and colloids 24 (2008) 1484-8.
[18] Y. Peng, Z. Wang, Tribological properties of sodium dodecyl sulfate aqueous dispersion of graphite-derived carbon materials, RSC Advances 4 (2014) 9980.
[19] S. Liang, Z. Shen, M. Yi, L. Liu, X. Zhang, S. Ma, In-situ exfoliated graphene for high-performance water-based lubricants, Carbon 96 (2015).
[20] K. Gao, Q. Chang, B. Wang, R. Gao, J. He, Preparation of Fe3O4@C composite nanoparticles with core-shell structure in subcritical water condition, Diamond and Related Materials 101 (2020) 107627.
[21] X. Li, Q. Zhou, Y. Huang, J. Yang, Nanoindentation and abrasion in Fe3O4/rGO reinforced epoxy electromagnetic protective coatings, Journal of Alloys and Compounds 887 (2021) 161277.
[22] Y. Xu, J. Geng, Y. Peng, Z. Liu, J. Yu, X. Hu, Lubricating mechanism of Fe3O4@MoS2 core-shell nanocomposites as oil additives for steel/steel contact, Tribology International 121 (2018) 241-251.
[23] Q. Zhang, H. Song, B. Wu, W. Feng, X. Li, Y. Jiao, X. Hu, Effect of magnetic field on the tribological behaviors of Fe3O4@MoS2 as polyalphaolefin additive in the steel/steel friction interface, Wear 466-467 (2021) 203586.
[24] X. Zheng, Y. Xu, J. Geng, Y. Peng, D. Olson, X. Hu, Tribological behavior of Fe3O4/MoS2 nanocomposites additives in aqueous and oil phase media, Tribology International 102 (2016) 79-87.
[25] G. Zhou, Y. Zhu, X. Wang, M. Xia, Y. Zhang, H. Ding, Sliding tribological properties of 0.45% carbon steel lubricated with Fe3O4 magnetic nano-particle additives in baseoil, Wear 301(1) (2013) 753-757.
[26] L. Malard, M. Pimenta, G. Dresselhaus, M. Dresselhaus, Raman Spectroscopy in Graphene, Physics Reports-review Section of Physics Letters - PHYS REP-REV SECT PHYS LETT 473 (2009) 51-87.
[27] L.M. Malard, M.A. Pimenta, G. Dresselhaus, M.S. Dresselhaus, Raman spectroscopy in graphene,

Physics Reports 473(5) (2009) 51-87.
[28] C. Casiraghi, A.C. Ferrari, J. Robertson, Raman spectroscopy of hydrogenated amorphous carbons, Physical Review B 72(8) (2005) 085401.
[29] A.C. Ferrari, J. Meyer, V. Scardaci, C. Casiraghi, M. Lazzeri, F. Mauri, S. Piscanec, D. Jiang, K. Novoselov, S. Roth, A.K. Geim, Raman Spectrum of Graphene and Graphene Layers, Physical review letters 97 (2006) 187401.
[30] S. Ramya, N. Gopala Krishna, K. Mudali, In-situ Raman and X-ray photoelectron spectroscopic studies on the pitting corrosion of modified 9Cr-1Mo steel in neutral chloride solution, Applied Surface Science 428 (2017).
[31] X.-M. Liu, S.-Y. Fu, H.-M. Xiao, Fabrication of octahedral magnetite microcrystals, Materials Letters 60 (2006) 2979-2983.
[32] W. Zhang, L. Gai, Z. Li, H. Jiang, W. Ma, Low temperature hydrothermal synthesis of octahedral Fe3O4 microcrystals, Journal of Physics D: Applied Physics 41 (2008) 225001.
[33] L. Wu, L. Gu, R. Jian, Lubrication mechanism of graphene nanoplates as oil additives for ceramics/steel sliding components, Ceramics International (2021).
[34] Z. Zhang, Y. Guo, F. Han, D. Wang, S. Zhang, Multilayer graphene for reducing friction and wear in water-based sand cleaning liquid, Wear 470-471 (2021) 203619.
[35] L. Wang, A.K. Tieu, G. Hai, J. Li, H. Zhu, T.P. Sang, J. Yang, Na2CO3 and graphene nanocomposites toward efficient lubrication, Carbon 177 (2021) 138-150.
[36] S. Zhang, C. Zhang, Y. Hu, L. Ma, Numerical simulation of mixed lubrication considering surface forces, Tribology International 140 (2019) 105878.
[37] Y. Fang, L. Ma, J. Luo, Modelling for water-based liquid lubrication with ultra-low friction coefficient in rough surface point contact, Tribology International 141 (2020) 105901.
[38] J.O.N. Wonham, Effect of Pressure on the Viscosity of Water, Nature 215(5105) (1967) 1053-1054.
[39] Y. Li, S. Li, P. Bai, W. Jia, Q. Xu, Y. Meng, L. Ma, Y. Tian, Surface wettability effect on aqueous lubrication: Van der Waals and hydration force competition induced adhesive friction, Journal of Colloid and Interface Science 599 (2021) 667-675.
[40] Z. Pawlak, W. Urbaniak, A. Oloyede, The relationship between friction and wettability in aqueous environment, Wear 271(9) (2011) 1745-1749.
[41] Z. Wu, C. Sheng, Z. Guo, Y. Li, R. Malekian, Z. Li, Surface texture processing for tribological performance improvement of UHMWPE-based water-lubricated bearings, Industrial Lubrication and Tribology 70(7) (2018) 1341-1349.
[42] S. Singh, X. Chen, C. Zhang, R. Tyagi, J. Luo, Investigation on the lubrication potential of graphene oxide aqueous dispersion for self-mated stainless steel tribo-pair, Vacuum 166 (2019) 307-315.